UCLA

Title

Early pregnancy imaging predicts ischemic placental disease.

Permalink

Authors

Lee, Brian
Aliabadi, Arya
Lei, Margarida
et al.

Publication Date

DOI

Early Pregnancy Imaging Predicts Ischemic Placental Disease

Brian Lee, MD[**,a,1], **Carla Janzen, MD, PhD**[**,b], **Arya R. Aliabadi, MD**[b,2], **Margarida Y. Y. Lei**[b], **Holden Wu, PhD**[d], **Dapeng Liu, PhD**[d,3], **Sitaram S. Vangala**[e], **Sherin U. Devaskar, MD**[a,*], **Kyunghyun Sung, PhD**[d]

[a]Department of Pediatrics, David Geffen School of Medicine, University of California, Los Angeles, CA, USA; 10833 Le Conte Ave, Los Angeles, CA 90095;

[b]Department of Obstetrics and Gynecology, David Geffen School of Medicine, University of California Los Angeles, USA; 10833 Le Conte Ave, Los Angeles, CA 90095;

[d]Department of Radiological Sciences, David Geffen School of Medicine, University of California, Los Angeles, CA, USA; 300 Medical Plaza, B119, Los Angeles, CA 90095;

[e]Department of Medicine Statistical Core, David Geffen School of Medicine, University of California, Los Angeles, CA, USA; 1100 Glendon Ave Suite 1820, Los Angeles, CA 90095;

Abstract

Introduction—To characterize early-gestation changes in placental structure, perfusion, and oxygenation in the context of ischemic placental disease (IPD) as a composite outcome and in individual sub-groups.

Methods—In a single-center prospective cohort study, 199 women were recruited from antenatal clinics between February 2017 and February 2019. Maternal magnetic resonance imaging (MRI) studies of the placenta were temporally conducted at two timepoints: 14–16 weeks gestational age (GA) and 19–24 weeks GA. The pregnancy was monitored via four additional study visits, including at delivery. Placental volume, perfusion, and oxygenation were assessed at both MRI timepoints. The primary outcome was defined as pregnancy complicated by IPD, with group assignment confirmed after delivery.

Results—In early gestation, mothers with IPD who subsequently developed fetal growth restriction (FGR) and/or delivered small-for gestational age (SGA) infants showed significantly decreased MRI indices of placental volume, perfusion, and oxygenation compared to controls. The prediction of FGR or SGA by multiple logistic regression using placental volume, perfusion, and

* **Corresponding Author and Reprint Requests to:** Sherin U. Devaskar, M.D., Department of Pediatrics, David Geffen School of Medicine, University of California, Los Angeles, CA, USA, SDevaskar@mednet.ucla.edu, Fax: 1-424-901-0006.
** Co-First Authors with Equal Contributions to the Study Manuscript.
[1] Present Address: Kaiser Permanente Panorama City Medical Center, 13651 Willard St., Panorama City, CA 91402
[2] Present Address: Department of Obstetrics, Gynecology & Reproductive Sciences, University of California, San Francisco, 490 Illinois St, 10th fl, Box #1032, San Francisco, CA 94143
[3] Present Address: Department of Radiology, Division of MR Research, Johns Hopkins University, 707 North Broadway, Baltimore, MD 21205

oxygenation revealed receiver operator characteristic curves with areas under the curve of 0.81 (Positive predictive value (PPV) = 0.84, negative predictive value (NPV) = 0.75) at 14–16 weeks GA and 0.66 (PPV = 0.78, NPV = 0.60) at 19–24 weeks GA.

Discussion—MRI indices showing decreased placental volume, perfusion and oxygenation in early pregnancy were associated with subsequent onset of IPD, with the greatest deviation evident in subjects with FGR and/or SGA. These early-gestation MRI changes may be predictive of the subsequent development of FGR and/or SGA.

Keywords

Placental blood flow; oxygenation; perfusion; ischemic placental disease

Introduction

Ischemic placental disease (IPD), caused by the failure of physiologic transformation of the maternal uterine spiral arteries, clinically manifests as preeclampsia (PE), fetal growth restriction, placental abruption, or a combination of these conditions, and is responsible for over half of medically indicated premature births [1–4]. Fetuses affected by IPD suffer from an increased risk of perinatal morbidity, mortality, and risk for long-term adverse health effects [5–13]. Fetal growth restriction (FGR) is diagnosed when the growth of the fetus does not reach its genetic potential [14].

During the first trimester, a system of villous trees proliferates by branching angiogenesis and lacunae are transformed into the intervillous space of the placenta [15]. At the end of the first trimester, maternal arterial circulation is established, and the highly branched chorionic villous trees provide efficient maternal-fetal diffusion. Around 20 weeks' gestation and onwards, there is exponential elaboration of the peripheral placental circulation with formation of intermediate and terminal villi. Subsequently, in the last trimester of pregnancy, nonbranching angiogenesis elongates capillaries with creation of parallel circuits, maximizing oxygen transport to the fetus [16, 17], thereby gradually decreasing resistance to blood flow in fetal umbilical arteries. By 24 weeks gestation, the maternal spiral arteries have fully converted to low resistance vessels. When this does not occur, as in pregnancies complicated by severe FGR, the fetal umbilical arteries and the maternal uterine arteries may demonstrate increased resistance when measured by Doppler ultrasound.

Studies of uteroplacental perfusion by ultrasound Doppler measurements of the uterine artery have shown increased resistive indices to placental perfusion in IPD [18, 19], but have yielded only moderate sensitivities in the prediction of IPD, and have not shown consistent benefit in improving the pregnancy or fetal outcome [20, 21]. Uterine artery Doppler measurement after mid-gestation (20–24 weeks) occurs at a time when severe IPD is often already clinically diagnosable and interventions are too late.

Changes in early-gestation placental perfusion may be better assessed directly using magnetic resonance imaging (MRI), which has shown the feasibility of accessing differences in placental oxygenation and perfusion between mothers with a normal pregnancy and those who developed IPD [22–26]. However, this has not been extensively studied in

early gestation, when the window for future development of potential interventions may be most optimal. The purpose of this study is to investigate the feasibility of using MRI measurements for the prediction of the subsequent development of IPD. We hypothesized that placental volume, perfusion, and oxygenation would be reduced in patients who develop IPD when compared to patients with a normal pregnancy. Non-invasive MRI measurements of the placenta during early gestation prior to the clinical manifestations of the disease may be predictive of the development of IPD and its associated morbidities particularly FGR/SGA. We performed MRI at the end of the first trimester and at the middle of the second trimester, which correlate with key physiological changes in angiogenesis that affect vascular development in placenta. We aimed to identify women prior to 24 weeks, so that necessary measures such as close surveillance monitoring can be initiated early enough to improve outcomes.

Further, the aim of this study was to establish the feasibility of MRI imaging in pregnancy and assess high resolution measurement of placental perfusion *in vivo* during early gestation, prior to the clinical diagnosis of IPD. This is a time of angiogenesis that has eluded analysis by ultrasound Doppler evaluation.

Materials and Methods

Patient Recruitment and Data Collection

This is a single-center prospective study approved by the University of California Los Angeles (UCLA) Institutional Review Board (IRB#:15–001388). Informed consent was provided by all subjects upon recruitment, and the study was registered in clinicaltrials.gov as #NCT02786420. All subjects were part of the Human Placenta Project [27], an NIH-initiated longitudinal study to understand placental structure and function changes in-vivo throughout pregnancy, and how these changes lead to different maternal and neonatal outcomes.

A total of 199 women were prospectively recruited from established UCLA antenatal clinics without pre-selection criteria for high-risk factors (Figure 1). The subjects were consented between February 2017 and February 2019 for participation in the study at the UCLA Ronald Reagan Medical Center. Inclusion criteria included a maternal age of more than 18 years with the ability to provide consent, gestational age less than 14 weeks, a singleton pregnancy, the absence of fetal structural or chromosomal abnormalities in the first trimester, maternal non-smoking status, and a plan to deliver at the same local institution. Exclusion criteria included maternal age less than 18 years, fetal malformation or chromosomal abnormality discovered at any time during the study, twin pregnancy, a plan to terminate the pregnancy, or the inability to provide consent.

Maternal information including age, pre-pregnancy body mass index (BMI), and prior pregnancy history were recorded at recruitment. Research activities including detailed survey questionnaires were integrated into the timeline of routine patient care prospectively via 4 planned study visits: the first at a gestational age of 11 – 14 weeks, the second at 20 – 29 weeks, the third at 36 weeks, and the fourth at delivery. The subjects also underwent two MRI studies, in separate visits from the study visits, temporally at two timepoints: 14 –

16 weeks gestational age (GA) at the first timepoint, and 19 – 24 weeks GA at the second timepoint.

The development of IPD was part of routine diagnosis by frontline clinicians in our academic medical center, confirmed by the investigators (with Maternal-Fetal Medicine expertise) via chart audits after delivery. For this study, the primary outcome of IPD was a composite defined as the subject developing at least one of the following outcomes at any time in pregnancy: preeclampsia, fetal growth restriction, or an SGA infant birth, according to ACOG definitions [28–31]. Preeclampsia was defined as a blood pressure greater than 140/90 on two separate occasions at least four hours apart, after 20 weeks' gestation, with a previously normal blood pressure, and proteinuria greater than or equal to 300mg/24 hours. In the absence of proteinuria, preeclampsia was defined as a new-onset hypertension with a new-onset thrombocytopenia, renal insufficiency (as defined by serum creatinine greater than 1.1mg/dL), impaired liver function (elevated liver transaminitis at least twice the normal values), pulmonary edema, or cerebral or visual symptoms [30]. At our institution, pregnancies are routinely screened for fetal growth restriction (FGR) in the third trimester by fundal height measurements, and by ultrasound performed by a Maternal-Fetal Medicine Specialist at approximately 30–34 weeks gestation. Fetal growth restriction (FGR) was a prenatal diagnosis defined as a fetus with an estimated fetal weight or abdominal circumference less than the 10th percentile for gestational age by ultrasound [31] using the Hadlock population-based fetal growth reference [32], and clinically managed per SMFM guidelines [29]. Small for gestational age (SGA) was a postnatal diagnosis defined as a birth weight less than the 10th percentile for gestational age, per Fenton's sex-specific growth charts [33, 34]. Neonatal outcomes were recorded at delivery, and neonates were followed up to 16 weeks after birth.

The subjects were further stratified into BMI categories in terms of their pre-pregnancy BMI, measured in kg/m^2. A BMI less than 18.5 was underweight; greater than 18.5 but less than 25 was normal weight; greater than or equal to 25 but less than 30 was overweight and greater than or equal to 30 was obese.

MRI Acquisition and Image Analysis for Placental Volume, Perfusion, and Oxygenation (Figure 2)

The placenta MRI protocol includes T2-weighted (T2w) MRI for placenta volume measurement, pseudo-continuous arterial spin labeling (pCASL) for placenta perfusion [25, 26], and a multi-echo gradient echo sequence for placenta oxygenation [27] which were developed as part of the NIH-initiated Human Placenta Project [27]. Technical aspects of the MRI acquisition protocols and image analysis have been previously published [23, 35]. All image analyses were performed after the completion of the subject recruitment in a blinded fashion to the pre-pregnancy history, clinical presentation and the study outcome.

The outcomes we evaluated were placental volume, placental perfusion, and placental oxygenation. Placental volume was measured in cubic centimeters. Placental perfusion measured the maternal arterial blood flow to the placenta in milliliters/100 grams/minute, as mean maternal placental blood flow throughout the entire placenta (MPBF; maternal placental blood flow), and areas of maternal high placental blood flow (MhPBF), a new

imaging parameter of showing the existent heterogeneity of MPBF [25, 26]. Placental oxygenation measured blood hemoglobin saturation within the placenta, recorded as R2* measurements. A *decrease* in blood hemoglobin saturation was inferred by an *increased* value of the R2* measurement which assessed deoxygenated hemoglobin [24]. Results were reported as the average R2* throughout the entire placenta, as well as the average value of the top 25th percentile of R2* measurements (average top 25% R2*).

Power Analysis

A power analysis was undertaken prior to the initiation of the clinical trial designed to obtain an overall 80% power with a significance at $p < 0.05$, resulting in our planned sample size consisting of recruiting around 200 subjects with an expected incidence of IPD of 10% [33], and an incidence of IPD with associated FGR and/or SGA of 5% [33].

Statistical Analysis

GraphPad Prism 9 (Dotmatics, Boston, Massachusetts) was used to perform statistical analysis. Independent-sample t test and Chi-squared test were used to compare outcomes between groups. A p-value less than or equal to 0.05 was considered significant. Multiple logistic regression analyses to create receiver operating characteristic (ROC) curves were also performed using Prism 9. Positive predictive values (PPV) and negative predictive values (NPV) were calculated using the sensitivity and specificity at the maximum Youden's Index of the ROC curve.

Results

Participants and Study Demographics

199 subjects were recruited in the first trimester of pregnancy. 18 women were not included in this analysis for various reasons, including no MRI performed, a loss to follow-up, or fetal demise. There was a total of 181 women remaining for analysis (Figure 1). Maternal characteristics are shown in Table 1. Of those 181 women, 151 women (83.0%) had a pregnancy unaffected by IPD, forming our control group; and 30 women (17.0%) developed IPD during pregnancy forming our IPD group. Within the IPD group, 17 (9%), women developed PE (3 with FGR), 11 women (6.0%) developed FGR, and an additional 5 subjects had newborns diagnosed with SGA alone (pregnancies not prenatally diagnosed with FGR); thus, the subgroup analysis of FGR and SGA (FGR+SGA) within the IPD group totaled 16 subjects (Table 2). None of the FGR/SGA group developed abnormal umbilical artery (UA) measurements. We observed 4 subjects who had preeclampsia with severe features (3 with FGR/SGA are included in Table 2, in addition to a fourth subject diagnosed with PE at 32 weeks' gestation). Overall, of the preeclampsia cases (n=17), two subjects developed early (<34 weeks) preeclampsia, and the remainder were diagnosed after 34 weeks. The majority of the subjects, other than the 3 with PE + FGR/SGA overlap, developed late, mild preeclampsia, without FGR/SGA. There were no cases of placental abruption. Based on the actual incidence observed in our recruited cohort of subjects, that is 30 patients developed IPD, we achieved a power of 83% in our analysis for the outcome of IPD. PE alone, FGR+SGA, and PE + FGR/SGA subgroup analyses were also performed.

Placental Volume Analysis (Table 3)

At the first MRI timepoint (14 – 16 weeks GA), the mean placental volume was significantly reduced in the IPD subjects who developed FGR or had an SGA delivery (FGR+SGA), as compared to the control group (FGR+SGA: 115.4 ± 28.1 cm^3, n = 16; controls: 138.9 ± 47.6 cm^3, n = 147, p < 0.05). The mean placental volumes were lower, but not significantly different when comparing either all subjects who developed IPD, or the subgroup of subjects who developed fetal growth restriction, preeclampsia, and had a small for gestational age birth (FGR+SGA+PE), to the control group (IPD: 136.5 ± 49.9 cm^3, n = 30; FGR+SGA+PE: 100.2 ± 28.7, n = 3, p = 0.16).

At the second MRI timepoint (19 – 24 weeks GA), the mean placental volumes were significantly reduced in the FGR+SGA subgroup of IPD as well as the FGR+SGA+PE subgroup, as compared to the control group (FGR+SGA: 221.9 ± 66.3 cm^3, n = 15; controls: 263.4 ± 72.7 cm^3; p < 0.05; FGR+SGA+PE: 178.7 ± 40.0 cm^3, n = 3, p < 0.05). The mean placental volumes were not significantly different in the overall IPD group as compared to the control group (IPD: 273.2 ± 95.3 cm^3, n = 28, p = 0.62).

Placental Perfusion Analysis (Table 3)

At the first MRI timepoint (14 – 16 weeks GA), mean MPBF values were lower, but not significantly different in either the IPD group, FGR+SGA subgroup, or FGR+SGA+PE subgroup, when compared to the control group (IPD: 58.4 ± 19.3, n = 28, p = 0.17; FGR+SGA: 55.8 ± 19.5, n = 15, p = 0.14; controls: 64.4 ± 21.5, n = 147; FGR+SGA+PE: 50.6 ± 16.7, n = 3, p = 0.27).

Areas of MhPBF were separately measured and showed significantly decreased mean values in the FGR+SGA subgroup when compared to the control group (FGR+SGA: 167.7 ± 67.7, n = 15; controls: 231.1 ± 104.8, n = 147; p < 0.05). The mean value of MhPBF in the IPD group was significantly decreased compared to the control group (IPD: 182.3 ± 86.0, n = 28; p < 0.05). The mean MhPBF was also decreased, but not statistically significant, in the FGR+SGA+PE subgroup (FGR+SGA+PE: 150.3 ± 55.9, p = 0.19).

At the second MRI timepoint (19 – 24 weeks GA), both mean MPBF and MhPBF revealed no significant differences in the IPD group overall, or in the FGR+SGA or FGR+SGA+PE subgroups, when compared to the control group. MPBF values were not significantly different in either the FGR+SGA subgroup or IPD group when compared to the control group (IPD: 71.2 ± 25.0, n = 26, p = 0.92; FGR+SGA: 67.1 ± 25.1, n = 15, p = 0.59; FGR+SGA+PE: 73.0 ± 49.4, n = 3, p = 0.96; vs. controls: 72.0 ± 33.9, n = 139). MhPBF values were not significantly different in the IPD group, or FGR+SGA or FGR+SGA+PE subgroups, when compared to the control group (IPD: 241.0 ± 108.3, n = 26, p = 0.64; FGR+SGA: 222.4 ± 100.3, n = 15, p = 0.37; FGR+SGA+PE: 207.6 ± 114.4, n = 3, p = 0.55; vs. controls: 253.7 ± 131.2, n = 139).

Placental Oxygenation Analysis (Table 3)

At the first MRI timepoint (14 – 16 weeks GA), the average R2* was significantly increased for both the FGR+SGA and FGR+SGA+PE subgroups of IPD, when compared to the

control group (FGR+SGA: 22.1 ± 6.6 s^{-1}, n = 14, p < 0.05; FGR+SGA+PE: 30.1 ± 5.4 s^{-1}, n = 3, p < 0.05; controls: 18.3 ± 5.3 s^{-1}, n = 124). R2* is known to increase due to local field inhomogeneities caused by increasing deoxyhemoglobin, the form of hemoglobin without oxygen (24). In the IPD group, the average R2* patterned higher without statistical significance as compared to the control group (IPD: 20.6 ± 6.3 s^{-1}, n = 23; controls: 18.3 ± 5.3 s^{-1}, n = 124, p < 0.10). The average top 25% R2* values were significantly increased for the FGR+SGA group when compared to the control group (FGR+SGA: 31.7 ± 11.6 s^{-1}, n = 14; controls: 25.6 ± 9.2 s^{-1}, n = 124; p < 0.05). The average top 25% R2* values showed a pattern of increase in both the IPD group and the FGR+SGA+PE subgroup when compared to the control group (IPD: 29.2 ± 10.3 s^{-1}, n = 23, p < 0.10; FGR+SGA+PE: 49.5 ± 7.0 s^{-1}, n = 3, p < 0.10; controls: 25.6 ± 9.2 s^{-1}, n = 124).

At the second MRI timepoint (19 – 24 weeks GA), there was a significant increase in the average R2* in FGR+SGA+PE subgroup when compared to the control group (FGR+SGA+PE: 30.3 ± 19.7 s^{-1}, n = 3, p < 0.05; vs. controls: 18.5 ± 5.0 s^{-1}, n = 122). There was a pattern of increase in average R2* in the FGR+SGA subgroup rather than the IPD group when compared to the control group (FGR+SGA: 20.7 ± 9.6 s^{-1}, n = 15, p = 0.16; IPD: 19.6 ± 7.8 s^{-1}, n = 24, p = 0.36), not reaching statistical significance. There was a pattern of increase in the average top 25% R2* values in the FGR+SGA subgroup, but not in the FGR+SGA+PE subgroup, and IPD group when compared to the control group (FGR+SGA: 28.7 ± 15.1 s^{-1}, n = 15, p = 0.10; FGR+SGA+PE: 44.8 ± 32.0 s^{-1}, n = 3, p = 0.35; IPD: 27.5 ± 12.2 s^{-1}, n = 24, p = 0.19; controls: 25.3 ± 6.2 s^{-1}, n = 122), with all three not reaching statistical significance.

Prediction Modeling Using Multiple Logistic Regression Analyses

Multiple logistic regression analyses were performed for the outcome of developing any condition of IPD, as well as for the outcome of FGR + SGA, using MRI-assessed placental volume, MPBF, MhPBF, R2*, and average top 25% R2* combined, to create ROC curves at MRI timepoints 14 – 16 weeks and 19 – 24 weeks GA (Figure 3).

When the analysis was performed specifically for the outcome of FGR or SGA (n=16), the area under the curve (AUC) for the ROC curve at the first timepoint of 14 – 16 weeks was 0.81 (p<0.01), and at 19 – 24 weeks the AUC was 0.66 (p=0.04). The PPV of FGR or SGA at the first and second time points were 0.84 and 0.78, respectively. The NPV of FGR or SGA at the first and second time points were 0.75 and 0.60, respectively (Table 4).

For the outcome of any condition of IPD, the AUC for the ROC curve was 0.72 (p<0.01) for the first timepoint, and 0.59 (p=0.22) for the second timepoint. The PPV of IPD at the first and second time points were 0.68 and 0.55, respectively. The NPV of IPD at the first and second time points were 0.75 and 0.70, respectively.

As increased BMI is a risk factor for ischemic placental disease [36], we stratified the control group, IPD group, and IPD subgroups into underweight, normal-weight, overweight, and obese subgroups. When comparing controls of a BMI subgroup against the same BMI subgroup of patients with IPD, we continued to see the same patterns in placental volumes, perfusion, and oxygenation in the IPD patients, at both MRI timepoints, despite the even

smaller sample sizes in each BMI category. Thus, the BMI of a pregnant subject may not have affected the perturbed placental features that emerged either due to IPD alone or with FGR + SGA. Since pre-pregnancy BMI categories presented results no different from each other, all categories of BMI were combined and presented in the results. Similarly, inclusion or exclusion of gestational diabetes mellitus (GDM) in controls and the IPD groups did not affect the overall results due to a similar prevalence in both groups (p=0.8).

Discussion

IPD adversely affects the short- and long-term health of both the mother and her fetus. MRI studies in early pregnancy have been shown to be safe for the fetus [37], and have shown promise in providing insights into the placental structure, perfusion, and oxygenation [38].

In this study, we characterized early-gestational placental changes in terms of placental volume, perfusion, and oxygenation. It is the first study to combine these three parameters into a comprehensive model of the developing and thereby changing placenta in early gestation, in the context of both normal pregnancies, pregnancies affected by IPD overall, and pregnancies with IPD that developed FGR + SGA. For this discussion, we address the changes seen across all IPD subjects, and in particular, focused on the IPD subgroup that presented with FGR + SGA.

In our study, we find that the IPD subgroup ultimately yielding FGR + SGA infants showed the greatest deviation from the control group in placental volume, perfusion, and oxygenation. Compared to the control group, placental volumes were significantly smaller, there was a pattern of lower placental perfusion with reduced high placental perfusion, and placental oxygenation was significantly decreased at the first MRI time point. While patients with FGR + SGA had the greatest placental alterations from our control group, comparing all IPD patients to our control group revealed similar patterns, albeit milder and not always significant, with placental volumes, perfusion and oxygenation. This is consistent with a relative failure of the normal vascular expansion that occurs in healthy pregnancy.

Overall, the first MRI at 14 – 16 weeks GA demonstrated more significant changes when compared to the second MRI. As predicted due to the abnormal vascular development of the placenta in patients who develop IPD, the pattern of changes at the first time point showed decreased placental volume, perfusion, and oxygenation in subjects who developed IPD. A decrease in placental volume and perfusion from the maternal circulation likely led to the significantly reduced placental oxygenation. This significant decrease in placental perfusion is not observed at the second time point. However, patients who develop FGR and have an SGA delivery continue to show significantly reduced placental volumes at the second time point, and patients who develop FGR, SGA, and preeclampsia have both significantly reduced placental volumes and oxygenation at the second time point, as well.

These observations are highly suggestive of the possibility of risk stratifying subjects for closer surveillance monitoring based on earlier gestational MRI biomarkers, rather than later ones. Additionally, while placental changes seen in the entire IPD group may not have all shown significance at the first MRI timepoint, the IPD subgroup that ultimately yielded FGR

+ SGA infants could be risk stratified at 14 – 16 weeks GA based on placental features even prior to the emergence and detection of FGR by fetal imaging. Such risk stratification can prove helpful in future studies of testing interventions in addition to undertaking close surveillance monitoring.

Our findings reflect our understanding of IPD as a chronic reduction in the delivery of maternal nutrient- and oxygen-rich blood to the placenta via the spiral arteries, which normally transform during the first trimester of pregnancy [39]. Not all IPD cases necessarily present with FGR or an SGA infant. In IPD, histological studies of the placenta after cesarean hysterectomy in women with PE, FGR, or hypertension, have shown a decreased number of fully-transformed spiral arteries when compared to a placenta from a normal pregnancy [40]. However, patients who developed FGR also had obstructive vascular lesions in the decidual and spiral arteries, which often lead to areas of placental ischemia [40]. Our present early-gestation study validated these subsequent clinical and pathological findings. Furthermore, the cellular and vascular mechanisms underlying the development of IPD is an early occurrence during pregnancy; however, FGR secondary to IPD is not seen until later in gestation, and in some cases ultimately culminating in the birth of an SGA infant.

In addition to the ability to risk-stratify subjects in early gestation, we explored the ability to predict both IPD and the subgroup of IPD with FGR or SGA. Our predictive modeling analysis showed that MRI-obtained values of placental volume, perfusion, and oxygenation, are able to predict the outcome of FGR + SGA particularly in early gestation, well before it manifests itself clinically during the late second and third trimesters. We see a similar potential predictive ability when evaluating all IPD subjects, although to a lesser extent. Most importantly, we find that the changes seen early in gestation at 14 – 16 weeks are the more highly predictive changes that herald the development of FGR + SGA. FGR + SGA carry significant adverse short-term health effects in the neonate, but the sequelae continue into childhood, manifesting as neurodevelopmental delay [5, 6], metabolic disorders [8–10], insulin resistance and type 2 diabetes [11], and cardiovascular disorders [12, 13]. The lifelong health implications across multiple systems for an infant born FGR + SGA set the individual for developing chronic non-communicable diseases with adverse effects on the quality of life. It is encouraging to be able to predict this eventuality prior to its occurrence during gestation, which may allow for testing earlier interventions towards improving outcomes.

Despite a similar size to the FGR +SGA cohort, we did not find significant differences in the subset with PE, unless there was also FGR + SGA. This may reflect the different clinical manifestations of IPD and in particular, preeclampsia (PE). Early-onset PE is highly associated with FGR and release of increased angiogenic markers, such as PlGF, whereas late-onset PE is rarely associated with FGR/SGA [41]. This has led to the proposal that there are 2 forms of PE, caused by differing degrees of impaired trophoblastic invasion. In the early form of PE, there is evidence that placental volume is reduced from as early as 12 weeks' GA, with premature onset of aberrant blood flow through the maternal spiral arteries into the central portions of the placenta. This dysfunctional establishment of maternal circulation may be a source of extreme oxidative stress, causing diverse outcomes from

miscarriage to preeclampsia, the latter in particular when reduced villous development does not lead to pregnancy loss [42]. The majority of the PE cohort in this investigation had late-onset PE, which likely reflected a milder degree of oxidative stress during placental development.

In this study, MRI parameters showed increased deoxygenation (top 25% of the R* which represents the highest levels of deoxyhemoglobin) in early pregnancy with FGR/SGA, consistent with reductions of high maternal blood flow (MhPBF). These differences may represent failure of maternal vascular expansion that likely pre-dates MRI evaluation at 14–16 weeks. Maternal blood flow and oxygenation were found to normalize at 19–24 weeks despite persistent decreased placental volume in these IPD with FGR+SGA pregnancies. Further investigation is needed to understand the way physiologic or pharmacologic adaptation to reduced blood flow may prevent the initiation of a pathological cascade leading to IPD.

The findings of our study are consistent with previous studies that have used MRI to evaluate placental function in IPD. Deloison et al. in 2021, using contrast-enhanced MRI in patients being evaluated for termination of pregnancy, showed a decrease in placental blood flow in pregnancies complicated by FGR, with MRI images performed from a rather wide range of 16 – 34 weeks' gestation [43]. Ho et. al in 2020 similarly showed that placental oxygenation, by means of T2*, was decreased in preeclamptic patients (one criterion for an IPD diagnosis) when compared to a gestation-matched control cohort, with MRI images performed in the second trimester and at delivery [44]. Unlike these two prior studies, our present investigation focused on an early gestation window using a combination of multiple MRI parameters.

In a previous study by our group [35], we found that women who developed gestational diabetes (GDM) patterned towards lower values of placental perfusion and higher values of placental volume. However, we analyzed our data without excluding GDM patients from both groups and found that the results were no different when comparing volume, perfusion, and oxygenation values between all controls and all patients who developed IPD. When comparing our present MRI studies to prior 3D ultrasound investigations (37, 38), we were able to capture placenta volumetric, perfusion (blood flow) and deoxygenation measurements with significant resolution early in pregnancy, while the previous ultrasound studies were able to assess the volume while employing chorionic measurements as surrogates rather than actually assessing placental blood flow. Despite these significant differences, it is reassuring at least with respect to placental volumes that the first imaging study was more predictive than the second study in both our MRI and the prior ultrasound study. Although, our ROC, PPV and NPV were far higher and more sensitive than with those reported previously by ultrasound measurements (37, 38).

Other ultrasound studies have focused on the uterine artery dimensions and blood flow measurements spanning from 20 weeks to 40 weeks gestation [45], while a separate study focused on these measurements during late first trimester until 28 weeks gestation [46]. While the values they obtained were in keeping with additional studies by other groups [47, 48], comparison between differing modalities of imaging can prove to be

challenging. Despite differences between ultrasound measurements of uterine artery blood flow (expressed as ml/min), and the pCASL MRI measured placental perfusion (MPBF and MhPBF) that accounts for only the maternal source of perfusion as in this present study (ml/100g/min), some comparisons can be drawn when placental weights at particular gestational ages [49] are featured into the calculations to derive the uterine artery blood flow per unit weight of the placenta, as was done with pCASL MRI imaging investigations.

More importantly, the predictive value of uterine artery blood flow measurement by ultrasound when compared to the predictive capabilities seen by early gestation MRI in our present study, the earlier time point of 14–16 weeks gestation revealed more robust prediction of the FGR+SGA sub-group of IPD than Uterine artery blood flow by ultrasound at this same gestation (33). When compared to mid-second trimester uterine artery Doppler and blood flow studies conducted previously [50], the predictive value of the MRI parameters during the same gestation was comparable, however the MRI during the earlier time point of 14–16 weeks in the present study performed far better. These observations and comparisons generate confidence that earlier MRI measurements of placental volume, perfusion and oxygenation at 14–16 weeks or even earlier in gestation may warrant further study. These MRI biomarkers may serve as a screening tool in certain stratified populations towards predicting the subsequent development of IPD with or without FGR/SGA.

Our study has strength in its prospective design. In addition, our subjects are representative of the general population as they were not selected based on any high-risk obstetrical factors or past medical history. The similarities between previously reported studies [45–50] and our present study are expected due to the pathophysiology of IPD; however, our MRI images were obtained earlier in gestation when compared to previous studies, and we show that placental changes are already apparent at much earlier timepoints. The later time point failing to show similar changes may reflect a vascular adaptation that occurs to overcome the ischemic insult experienced much earlier in gestation, or reflect complex pathophysiology related to aberrancy of blood flow through the spiral arteries during early gestation.

Our study has several limitations. First, the sample sizes for our IPD group and its subgroups are relatively small, reflecting the incidence of IPD in the general population. In addition, because of the small sample size, we safe guarded against the predictive model risking overfitting, by also employing a more parsimonious model (e.g., one with just the 3 individually strongest predictors), and found that the model performed nearly as well for FGR+SGA (0.79 v. 0.81), suggesting that our results do not entirely reflect the concern of overfitting.

Despite the relatively small sample sizes, however, our study was well-powered and we saw a consistent pattern in the changes in placental structure and function. In addition, our results are not separated by race or socioeconomic factors due to the limited sample sizes. We were also unable to conduct sub-group analyses of early onset versus late onset PE and/or FGR/SGA within the small sample size. Future multi-center prospective clinical trials involving other centers may increase the obstetric and pediatric confidence in the observations made in this study. A larger study would enhance the sample size of IPD with and without FGR and SGA, and further validate our present proof of concept, which will

have far-reaching implications affecting maternal health subsequent to the pregnancy and the entire life course of the offspring. Finally, current methods of stratifying patients by risk of developing adverse pregnancy outcomes include taking into account the patient's medical history, pregnancy history, and ultrasound Doppler studies, which are easier and less costly than an MRI study. However, our study shows the feasibility of MRI studies in the prediction of IPD, warranting further exploration of its utility, by itself or concurrent with ultrasound imaging.

In conclusion, pregnant women who develop IPD showed alterations in non-invasively MRI-assessed values of placental volume, perfusion, and oxygenation, as early as 14 weeks gestational age. The placental changes are seen across all clinical manifestations of IPD and are most significant in patients with IPD who develop FGR + SGA. Furthermore, we show these changes may be more predictive of the development of FGR + SGA. Our prospective study combines many of the capabilities of MRI in the evaluation of placental structure and function and expands the potential utility of MRI in early gestation towards the prediction of IPD, particularly when associated with FGR + SGA, and in the future, perhaps other adverse pregnancy outcomes. While currently no known interventions exist that are capable of reversing FGR, the results of our present investigation may provide a window of opportunity to study interventions prior to the emergence of IPD with FGR + SGA, setting the framework for future amelioration, if not reversal, of these conditions. Such amelioration strategies have the potential of improving the quality of life for the mother post-pregnancy and that of the offspring throughout the life course.

Data Availability:

Some or all datasets generated during and/or analyzed during the current study are not publicly available but are available from the corresponding author on reasonable request.

List of Abbreviations

AUC	area under the curve
BMI	body mass index
FGR	fetal growth restriction
GA	gestational age
GDM	gestational diabetes mellitus
MhPBF	maternal high placental blood flow
IPD	ischemic placental disease
MRI	magnetic resonance imaging
NPV	negative predictive values
MPBF	maternal placental blood flow
PE	preeclampsia
PPV	positive predictive values
ROC	receiver operating characteristic
SGA	small-for gestational age

References

[1]. Ananth CV. Ischemic placental disease: a unifying concept for preeclampsia, intrauterine growth restriction, and placental abruption. Semin Perinatol. 2014;38(3):131–2. doi: 10.1053/j.semperi.2014.03.001. [PubMed: 24836823]

[2]. Ananth CV, Peltier MR, Chavez MR, Kirby RS, Getahun D, Vintzileos AM. Recurrence of ischemic placental disease. Obstet Gynecol. 2007;110(1):128–33. Epub 2007/07/03. doi: 10.1097/01.AOG.0000266983.77458.71. [PubMed: 17601907]

[3]. Burton GJ, Jauniaux E. Pathophysiology of placental-derived fetal growth restriction. Am J Obstet Gynecol. 2018;218(2S):S745–S61. Epub 2018/02/10. doi: 10.1016/j.ajog.2017.11.577. [PubMed: 29422210]

[4]. Ananth CV, Vintzileos AM. Maternal-fetal conditions necessitating a medical intervention resulting in preterm birth. Am J Obstet Gynecol. 2006;195(6):1557–63. Epub 20061002. doi: 10.1016/j.ajog.2006.05.021. [PubMed: 17014813]

[5]. Murray E, Fernandes M, Fazel M, Kennedy SH, Villar J, Stein A. Differential effect of intrauterine growth restriction on childhood neurodevelopment: a systematic review. BJOG. 2015;122(8):1062–72. Epub 2015/05/21. doi: 10.1111/1471-0528.13435. [PubMed: 25990812]

[6]. Sacchi C, Marino C, Nosarti C, Vieno A, Visentin S, Simonelli A. Association of Intrauterine Growth Restriction and Small for Gestational Age Status With Childhood Cognitive Outcomes:

A Systematic Review and Meta-analysis. JAMA Pediatr. 2020;174(8):772–81. Epub 2020/05/27. doi: 10.1001/jamapediatrics.2020.1097. [PubMed: 32453414]

[7]. Ananth CV, Friedman AM. Ischemic placental disease and risks of perinatal mortality and morbidity and neurodevelopmental outcomes. Semin Perinatol. 2014;38(3):151–8. Epub 2014/05/20. doi: 10.1053/j.semperi.2014.03.007. [PubMed: 24836827]

[8]. Briana DD, Malamitsi-Puchner A. Intrauterine growth restriction and adult disease: the role of adipocytokines. Eur J Endocrinol. 2009;160(3):337–47. Epub 2008/12/20. doi: 10.1530/EJE-08-0621. [PubMed: 19095781]

[9]. Mericq V, Martinez-Aguayo A, Uauy R, Iniguez G, Van der Steen M, Hokken-Koelega A. Long-term metabolic risk among children born premature or small for gestational age. Nat Rev Endocrinol. 2017;13(1):50–62. Epub 2016/11/04. doi: 10.1038/nrendo.2016.127. [PubMed: 27539244]

[10]. Neitzke U, Harder T, Plagemann A. Intrauterine growth restriction and developmental programming of the metabolic syndrome: a critical appraisal. Microcirculation. 2011;18(4):304–11. Epub 2011/03/23. doi: 10.1111/j.1549-8719.2011.00089.x. [PubMed: 21418379]

[11]. Pinney SE, Simmons RA. Intrauterine Growth Restriction and Insulin Resistance. In: Zeitler PS, Nadeau KJ, editors. Insulin Resistance: Childhood Precursors of Adult Disease. Cham: Springer International Publishing; 2020. p. 239–53.

[12]. Cohen E, Wong FY, Horne RS, Yiallourou SR. Intrauterine growth restriction: impact on cardiovascular development and function throughout infancy. Pediatr Res. 2016;79(6):821–30. Epub 2016/02/13. doi: 10.1038/pr.2016.24. [PubMed: 26866903]

[13]. Syddall HE, Sayer AA, Simmonds SJ, Osmond C, Cox V, Dennison EM, et al. Birth weight, infant weight gain, and cause-specific mortality: the Hertfordshire Cohort Study. Am J Epidemiol. 2005;161(11):1074–80. Epub 2005/05/20. doi: 10.1093/aje/kwi137. [PubMed: 15901628]

[14]. Resnik R Intrauterine growth restriction. Obstet Gynecol. 2002;99(3):490–6. Epub 2002/02/28. doi: 10.1016/s0029-7844(01)01780-x. [PubMed: 11864679]

[15]. Turco MY, Moffett A. Development of the human placenta. Development. 2019;146(22). Epub 20191127. doi: 10.1242/dev.163428.

[16]. Jones CJ, Fox H. Ultrastructure of the normal human placenta. Electron Microsc Rev 1991;4(1):129–78. doi: 10.1016/0892-0354(91)90019-9. [PubMed: 1873486]

[17]. Kaufmann P Basic morphology of the fetal and maternal circuits in the human placenta. Contrib Gynecol Obstet. 1985;13:5–17. [PubMed: 3995983]

[18]. Khong SL, Kane SC, Brennecke SP, da Silva Costa F. First-trimester uterine artery Doppler analysis in the prediction of later pregnancy complications. Dis Markers. 2015;2015:679730. Epub 20150420. doi: 10.1155/2015/679730. [PubMed: 25972623]

[19]. Shahid N, Masood M, Bano Z, Naz U, Hussain SF, Anwar A, et al. Role of Uterine Artery Doppler Ultrasound in Predicting Pre-Eclampsia in High-Risk Women. Cureus. 2021;13(7):e16276. Epub 2021/08/12. doi: 10.7759/cureus.16276. [PubMed: 34377610]

[20]. Alfirevic Z, Stampalija T, Gyte GM. Fetal and umbilical Doppler ultrasound in high-risk pregnancies. Cochrane Database Syst Rev. 2010(1):CD007529. Epub 2010/01/22. doi: 10.1002/14651858.CD007529.pub2. [PubMed: 20091637]

[21]. Stampalija T, Gyte GM, Alfirevic Z. Utero-placental Doppler ultrasound for improving pregnancy outcome. Cochrane Database Syst Rev. 2010(9):CD008363. Epub 2010/09/09. doi: 10.1002/14651858.CD008363.pub2. [PubMed: 20824875]

[22]. Zhu MY, Milligan N, Keating S, Windrim R, Keunen J, Thakur V, et al. The hemodynamics of late-onset intrauterine growth restriction by MRI. Am J Obstet Gynecol. 2016;214(3):367 e1–e17. Epub 2015/10/18. doi: 10.1016/j.ajog.2015.10.004.

[23]. Armstrong T, Liu D, Martin T, Masamed R, Janzen C, Wong C, et al. 3D R 2 * mapping of the placenta during early gestation using free-breathing multiecho stack-of-radial MRI at 3T. J Magn Reson Imaging. 2019;49(1):291–303. Epub 2018/08/25. doi: 10.1002/jmri.26203. [PubMed: 30142239]

[24]. Huen I, Morris DM, Wright C, Parker GJ, Sibley CP, Johnstone ED, et al. R1 and R2 * changes in the human placenta in response to maternal oxygen challenge. Magn Reson Med. 2013;70(5):1427–33. Epub 2013/01/03. doi: 10.1002/mrm.24581. [PubMed: 23280967]

[25]. Liu D, Shao X, Danyalov A, Chanlaw T, Masamed R, Wang DJJ, et al. Human Placenta Blood Flow During Early Gestation With Pseudocontinuous Arterial Spin Labeling MRI. J Magn Reson Imaging. 2020;51(4):1247–57. Epub 2019/11/05. doi: 10.1002/jmri.26944. [PubMed: 31680405]

[26]. Shao X, Liu D, Martin T, Chanlaw T, Devaskar SU, Janzen C, et al. Measuring human placental blood flow with multidelay 3D GRASE pseudocontinuous arterial spin labeling at 3T. J Magn Reson Imaging. 2018;47(6):1667–76. Epub 2017/11/15. doi: 10.1002/jmri.25893. [PubMed: 29135072]

[27]. Guttmacher AE, Maddox YT, Spong CY. The Human Placenta Project: placental structure, development, and function in real time. Placenta. 2014;35(5):303–4. Epub 2014/03/26. doi: 10.1016/j.placenta.2014.02.012. [PubMed: 24661567]

[28]. ACOG Practice Bulletin No. 227: Fetal Growth Restriction: Correction. Obstet Gynecol. 2021;137(4):754. Epub 2021/03/25. doi: 10.1097/AOG.0000000000004350.

[29]. Society for Maternal-Fetal Medicine . Electronic address pso, Martins JG, Biggio JR, Abuhamad A. Society for Maternal-Fetal Medicine Consult Series #52: Diagnosis and management of fetal growth restriction: (Replaces Clinical Guideline Number 3, April 2012). Am J Obstet Gynecol. 2020;223(4):B2–B17. Epub 20200512. doi: 10.1016/j.ajog.2020.05.010.

[30]. Gestational Hypertension and Preeclampsia: ACOG Practice Bulletin, Number 222. Obstet Gynecol. 2020;135(6):e237–e60. doi: 10.1097/AOG.0000000000003891. [PubMed: 32443079]

[31]. Fetal Growth Restriction: ACOG Practice Bulletin Summary, Number 227. Obstet Gynecol. 2021;137(2):385–7. Epub 2021/01/23. doi: 10.1097/AOG.0000000000004252. [PubMed: 33481523]

[32]. Hadlock FP, Harrist RB, Martinez-Poyer J. In utero analysis of fetal growth: a sonographic weight standard. Radiology. 1991;181(1):129–33. doi: 10.1148/radiology.181.1.1887021. [PubMed: 1887021]

[33]. Janzen C, Lei MYY, Lee BR, Vangala S, DelRosario I, Meng Q, et al. A Description of the Imaging Innovations for Placental Assessment in Response to Environmental Pollution study (PARENTs). Am J Perinatol. 2022. Epub 2022/10/15. doi: 10.1055/a-1961-2059.

[34]. Fenton TR, Kim JH. A systematic review and meta-analysis to revise the Fenton growth chart for preterm infants. BMC Pediatr. 2013;13:59. Epub 20130420. doi: 10.1186/1471-2431-13-59. [PubMed: 23601190]

[35]. Lee B, Janzen C, Wu H, Vangala SS, Devaskar SU, Sung K. Utility of In-vivo Magnetic Resonance Imaging is Predictive of Gestational Diabetes Mellitus during Early Pregnancy. J Clin Endocrinol Metab. 2022. Epub 2022/10/18. doi: 10.1210/clinem/dgac602.

[36]. Parker SE, Werler MM. Epidemiology of ischemic placental disease: a focus on preterm gestations. Semin Perinatol. 2014;38(3):133–8. Epub 2014/05/20. doi: 10.1053/j.semperi.2014.03.004. [PubMed: 24836824]

[37]. Ray JG, Vermeulen MJ, Bharatha A, Montanera WJ, Park AL. Association Between MRI Exposure During Pregnancy and Fetal and Childhood Outcomes. JAMA. 2016;316(9):952–61. Epub 2016/09/07. doi: 10.1001/jama.2016.12126. [PubMed: 27599330]

[38]. Aughwane R, Ingram E, Johnstone ED, Salomon LJ, David AL, Melbourne A. Placental MRI and its application to fetal intervention. Prenat Diagn. 2020;40(1):38–48. Epub 2019/07/16. doi: 10.1002/pd.5526. [PubMed: 31306507]

[39]. Wang Y, Zhao S. Placental Blood Circulation. Vascular Biology of the Placenta. Integrated Systems Physiology: from Molecules to Function to Disease. San Rafael (CA)2010.

[40]. Brosens I, Pijnenborg R, Vercruysse L, Romero R. The "Great Obstetrical Syndromes" are associated with disorders of deep placentation. Am J Obstet Gynecol. 2011;204(3):193–201. Epub 2010/11/26. doi: 10.1016/j.ajog.2010.08.009. [PubMed: 21094932]

[41]. Rolnik DL, Wright D, Poon LCY, Syngelaki A, O'Gorman N, de Paco Matallana C, et al. ASPRE trial: performance of screening for preterm pre-eclampsia. Ultrasound Obstet Gynecol. 2017;50(4):492–5. Epub 20170824. doi: 10.1002/uog.18816. [PubMed: 28741785]

[42]. Burton GJ, Jauniaux E. Placental oxidative stress: from miscarriage to preeclampsia. J Soc Gynecol Investig. 2004;11(6):342–52. doi: 10.1016/j.jsgi.2004.03.003.

[43]. Deloison B, Arthuis C, Benchimol G, Balvay D, Bussieres L, Millischer AE, et al. Human placental perfusion measured using dynamic contrast enhancement MRI. PLoS One. 2021;16(9):e0256769. Epub 2021/09/03. doi: 10.1371/journal.pone.0256769. [PubMed: 34473740]

[44]. Ho AEP, Hutter J, Jackson LH, Seed PT, McCabe L, Al-Adnani M, et al. T2* Placental Magnetic Resonance Imaging in Preterm Preeclampsia: An Observational Cohort Study. Hypertension. 2020;75(6):1523–31. Epub 2020/04/28. doi: 10.1161/HYPERTENSIONAHA.120.14701. [PubMed: 32336233]

[45]. Acharya G, Wilsgaard T, Berntsen GK, Maltau JM, Kiserud T. Doppler-derived umbilical artery absolute velocities and their relationship to fetoplacental volume blood flow: a longitudinal study. Ultrasound Obstet Gynecol. 2005;25(5):444–53. doi: 10.1002/uog.1880. [PubMed: 15816007]

[46]. Assali NS, Rauramo L, Peltonen T. Measurement of uterine blood flow and uterine metabolism. VIII. Uterine and fetal blood flow and oxygen consumption in early human pregnancy. Am J Obstet Gynecol. 1960;79:86–98. doi: 10.1016/0002-9378(60)90367-7. [PubMed: 13794853]

[47]. Flo K, Wilsgaard T, Vartun A, Acharya G. A longitudinal study of the relationship between maternal cardiac output measured by impedance cardiography and uterine artery blood flow in the second half of pregnancy. BJOG. 2010;117(7):837–44. Epub 20100329. doi: 10.1111/j.1471-0528.2010.02548.x. [PubMed: 20353457]

[48]. Rigano S, Ferrazzi E, Boito S, Pennati G, Padoan A, Galan H. Blood flow volume of uterine arteries in human pregnancies determined using 3D and bi-dimensional imaging, angio-Doppler, and fluid-dynamic modeling. Placenta. 2010;31(1):37–43. Epub 20091127. doi: 10.1016/j.placenta.2009.10.010. [PubMed: 19945159]

[49]. Thompson JM, Irgens LM, Skjaerven R, Rasmussen S. Placenta weight percentile curves for singleton deliveries. BJOG. 2007;114(6):715–20. doi: 10.1111/j.1471-0528.2007.01327.x. [PubMed: 17516963]

[50]. Garcia B, Llurba E, Valle L, Gomez-Roig MD, Juan M, Perez-Matos C, et al. Do knowledge of uterine artery resistance in the second trimester and targeted surveillance improve maternal and perinatal outcome? UTOPIA study: a randomized controlled trial. Ultrasound Obstet Gynecol. 2016;47(6):680–9. doi: 10.1002/uog.15873. [PubMed: 26823208]

Highlights

- Free-breathing 3D MRI non-invasively measures placental perfusion and oxygenation

- Early gestation MRI biomarkers of the placenta are predictive of IPD with FGR+SGA

- IPD with FGR+SGA is heralded by reduced placental volume, perfusion and oxygenation
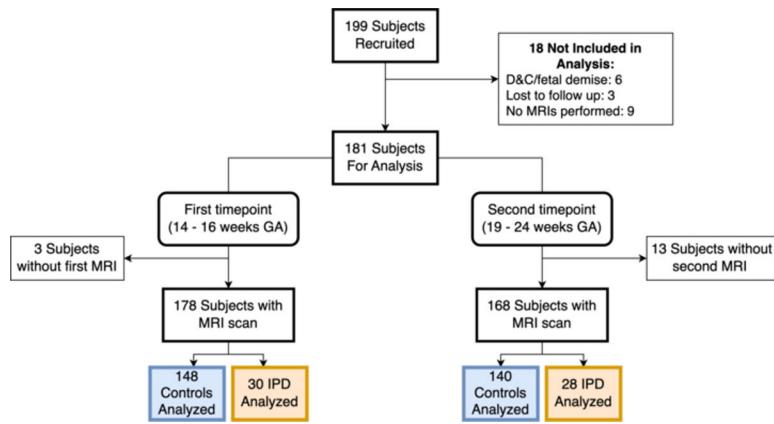
Figure 1.
Subject recruitment flowchart

D&C = dilatation and curettage; MRI = magnetic resonance imaging; GA = gestational age;

IPD refers to the ischemic placental disease group patients
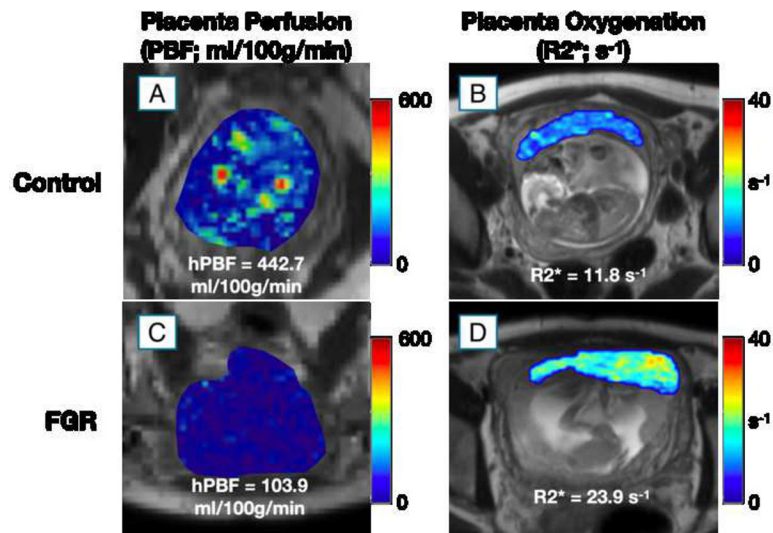
Figure 2.
Representative MRI Images of placental perfusion and oxygenation showing the clear visual difference in placental perfusion and oxygenation as obtained by MRI. Placental perfusion of a control patient at 16 0/7 weeks gestation (A, top left) has more areas of higher placental perfusion, as well as clear areas of high placental perfusion, when compared to a patient with ischemic placental disease manifesting as fetal growth restriction at 16 3/7 weeks gestation (FGR, C, bottom left), which shows low perfusion throughout the placenta. Placental oxygenation of the same control patient (B, top right), is increased, as evidenced by lower values of R2*, when compared to the same patient with FGR (D, bottom right). Higher R2* values indicate an increased amount of deoxygenated hemoglobin.
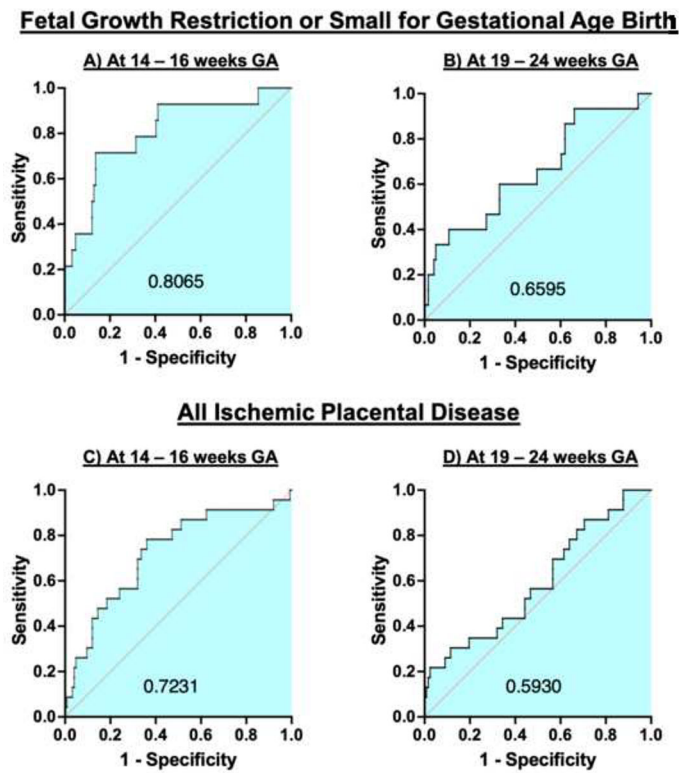
Figure 3.
Receiver operating curves for the prediction of fetal growth restriction or small for gestational age delivery, and ischemic placental disease overall. Numbers within the curves are the area under the curve: A) AUC=0.81 (p < .01), B) AUC=0.66 (p = 0.04), C) AUC=0.7231 (p<0.01), D) AUC= 0.593 (p=0.22).
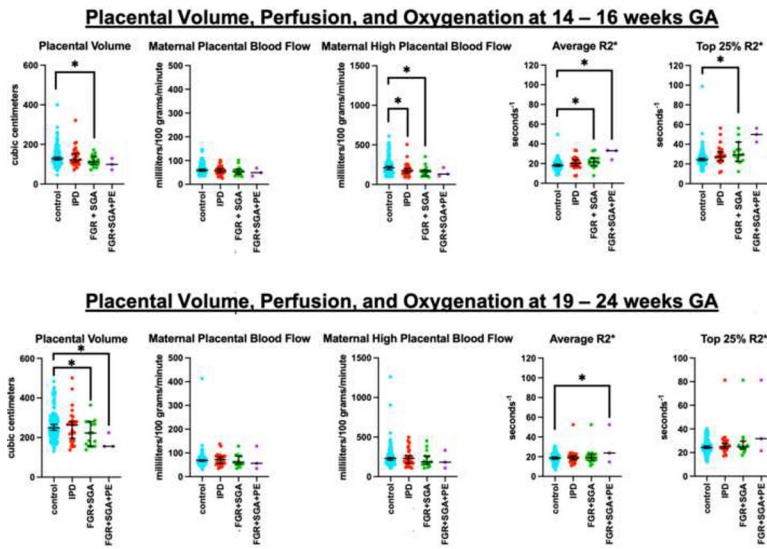
Figure 4:

Placental volume, perfusion, and oxygenation at 14 – 16 weeks gestational age (GA) and 19 – 24 weeks GA.

IPD: Ischemic placental disease group; FGR+SGA: fetal growth restriction and small for gestational age subgroup.

FGR+SGA+PE: Fetal growth restriction, small for gestational age, and preeclampsia subgroup. * = p < 0.05.

Table 1.

Self-reported maternal demographics

	Control	IPD (all)	FGR+SGA
N	151	30	16
Mean age at consent (years)	33.7 ± 4.3	34.4 ± 3.5	32.0 ± 5.5
p - value		0.39	0.14
GA at First MRI timepoint (weeks)	15.6 ± 1.0	16.0 ± 1.1	15.5 ± 1.1
p - value		0.09	0.53
GA at Second MRI timepoint (weeks)	20.8 ± 1.3	20.9 ± 0.9	20.4 ± 0.9
p - value		0.42	0.24
Race	Hispanic: 30	Hispanic: 5	Hispanic: 3
	White: 72	White: 14	White: 11
	Asian: 41	Asian: 8	Asian: 2
	Black: 7	Black: 4	Black: 0
	Native American: 1	Native American: 0	Native American: 0
	Control	**IPD (all)**	**FGR+SGA**
Parity	Multipara- 79 Nulipara - 72	Multipara- 13 Nulipara -17	Multipara- 6 Nulipara- 10
Multiparity with a history of IPD (n=9)	6/9 (67%)	3/9 (33%)	1/9 (11%)
p - value		0.1	0.55
BMI at consent (kg/m^2)	24.4 ± 4.5	24.6 ± 5.1	22.6 ± 2.8
p - value		0.86	0.10

IPD = ischemic placental disease; FGR+SGA = fetal growth restriction and small for gestational age; GA = gestational age; MRI = magnetic resonance imaging; BMI = body mass index; First MRI timepoint at 14 – 16 weeks GA; Second MRI timepoint at 19 – 24 weeks GA. P-values are compared to the control group for the respective variable. Data are shown as mean ± standard deviation.

Table 2.

Clinical Characteristics of FGR + SGA Pregnancies

	Gestational age at birth (wk)	Newborn Sex	Birth weight gm	Birth weight % (*)	Outcomes		
					Assignment	Antenatal	Postnatal
1	40w2d	Female	3118	23%	FGR	FGR: AC< 5% at 33 wks	Placental wt 385gm (<10%), Hypothermia
2	39w1d	Female	2720	11%	FGR	FGR: EFW <10% at 38 wks, Induction of labor for FGR.	Placental wt 332gm (<10%), Hypoglycemia
3	38w2d	Female	2930	33%	FGR	FGR: EFW <10% at 32wks.	Multiple placental thrombi, Hypoglycemia
4	37w1d	Female	2268	7%	FGR + SGA PE	FGR: EFW<10% at 29 weeks. Induction of labor for FGR. Severe preeclampsia	NICU Admission, Hypothermia
5	37w2d	Male	2170	3%	FGR + SGA	FGR: EFW<10% at 28 weeks. Induction of labor for FGR.	Placental wt 319gm (<10%)
6	40w3d	Male	3040	9%	SGA	Maternal anemia	
7	31w6d	Female	1135	8%	FGR + SGA PE	FGR: AC<5% at 28 wks, Severe preeclampsia at 29w3d, C/S for fetal distress.	NICU Admission, RDS
8	37w5d	Female	2353	7%	SGA		Placental wt 308gm (<10%)
9	41w0d	Female	2820	5%	SGA		Placental wt 343gm (<10%)
10	37w3d	Female	2185	5%	FGR + SGA PE	FGR: AC<5% at 33 wks, Severe preeclampsia at 37w2d, C/S for fetal distress.	NICU Admission
11	37w6d	Male	2790	11%	FGR	FGR: AC<6% at 34 wks, Gestational HTN.	
12	39w3d	Female	2690	8%	FGR + SGA	FGR: AC<4% at 37wks, Induction of labor for FGR.	
13	39w2d	Male	2900	12%	FGR	FGR: AC<5% at 39wks	
14	38w3d	Male	2620	8%	SGA		Placental wt 310gm (<10%)
15	38w0d	Female	2515	5%	FGR + SGA	FGR: EFW<10% at 34wks, Induction of labor for FGR.	
16	41w2d	Male	3232	9%	SGA		Placental wt 366gm (<10%)

FGR+SGA = fetal growth restriction and small for gestational age; GA = gestational age; wk = week; d = days; AC = abdominal circumference.PE = Preeclampsia.

(*)
Birth weight %centile by sex-specific Fenton population curves [34].

Table 3.

Summary of results of placental volume, perfusion, and oxygenation, at both MRI timepoints

		First MRI Timepoint (14 – 16 weeks GA)					Second MRI Timepoint (19 – 24 weeks GA)				
		Control	IPD (all)	FGR and SGA	PE	FGR and SGA and PE	Control	IPD (all)	FGR and SGA	PE	FGR and SGA and PE
Volume	N	147	30	16	16	3	140	28	15	16	3
	Mean ± SD	138.9 ± 47.6	136.5 ± 49.9	115.4 ± 28.1	149.9 ± 59.1	100.2 ± 28.7	263.4 ± 72.7	273.2 ± 95.3	221.9 ± 66.3	273.2 ± 95.3	178.7 ± 40.0
	P value [*]		p = 0.38	**p < 0.05**	p = 0.47	p = 0.16		p = 0.62	**p = 0.04**	p = 0.7	**p < 0.05**
MPBF	N	147	28	15	16	3	139	26	15	14	3
	Mean ± SD	64.4 ± 21.5	58.4 ± 19.3	55.8 ± 19.5	59.3 ± 18.9	50.6 ± 16.7	72.0 ± 33.9	71.2 ± 25.0	67.1 ± 25.1	76.0 ± 29.2	73.0 ± 49.4
	P value [*]		p = 0.17	p = 0.14	p = 0.32	p = 0.27		p = 0.92	p = 0.59	p = 0.63	p = 0.96
MhPBF	N	147	28	15	16	3	139	26	15	14	3
	Mean ± SD	231.1 ± 104.8	182.3 ± 86.0	64.4 ± 67.7	190.1 ± 96.9	150.3 ± 55.9	253.7 ± 131.2	241.0 ± 108.3	222.4 ± 100.3	253.8 ± 115.8	207.6 ± 114.4
	P value [*]		**p = 0.02**	**p = 0.02**	p = 0.14	p = 0.19		p = 0.64	p = 0.37	p = 0.99	p = 0.55
Average R2 [*]	N	124	23	14	12	3	122	24	15	12	3
	Mean ± SD	18.3 ± 5.3	20.6 ± 6.3	22.1 ± 6.6	21.2 ± 7.4	30.1 ± 5.4	18.5 ± 5.0	19.6 ± 7.8	20.7 ± 9.6	21.0 ± 10.4	30.3 ± 19.7
	P value [*]		p = 0.07	**p = 0.01**	p = 0.21	**p < 0.01**		p = 0.36	p = 0.16	p = 0.43	**p < 0.01**
Average Top 25% R2 [*]	N	124	23	14	12	3	122	24	15	12	3
	Mean ± SD	25.6 ± 9.2	29.2 ± 10.3	31.7 ± 11.6	31.3 ± 12.8	49.5 ± 7.0	25.3 ± 6.2	27.5 ± 12.2	28.7 ± 15.1	30.2 ± 16.6	44.8 ± 32.0
	P value [*]		p = 0.096	**p = 0.02**	p = 0.16	p = 0.07		p = 0.19	p = 0.10	**p = 0.03**	p = 0.35

[*]
p-values upon comparison to the corresponding control group value; significant if p ≤ 0.05

MRI = magnetic resonance imaging; GA = gestational age; IPD = ischemic placental disease; FGR and SGA = fetal growth restriction and small for gestational age; MPBF = maternal placental blood flow; MhPBF = maternal high placental blood flow; SD = standard deviation. Note the difference in n for some variables between the first and second MRI time points (example, n = 147 and n = 140 for the control group placental volume at the first and second MRI time points, respectively). These differences are the result of some subjects only obtaining one of the two MRI scans.

Table 4.

AUC, Sensitivity, Specificity, Positive Predictive Value, and Negative Predictive Value for Combined MRI Measurements of Placental Volume, Perfusion, and Oxygenation for the Outcome of Ischemic Placental Disease

Outcome		AUC (p-value)	Sensitivity	Specificity	PPV	NPV
14 – 16 weeks gestational age	IPD	0.72 (<0.01)	0.78	0.64	0.68	0.75
	FGR or SGA	0.81 (<0.01)	0.71	0.86	0.84	0.75
19 – 24 weeks gestational age	IPD	0.59 (0.22)	0.87	0.30	0.55	0.70
	FGR or SGA	0.66 (0.04)	0.40	0.89	0.78	0.60

AUC = area under the curve (p-value), PPV = positive predictive value, NPV = negative predictive value, IPD = ischemic placental disease, FGR = fetal growth restriction, SGA = small for gestational age